

"In presenting the dissertation as a partial fulfillment of the requirements for an advanced degree from the Georgia Institute of Technology, I agree that the Library of the Institution shall make it available for inspection and circulation in accordance with its regulations governing materials of this type. I agree that permission to copy from, or to publish from, this dissertation may be granted by the professor under whose direction it was written, or, in his absence, by the dean of the Graduate Division when such copying or publication is solely for scholarly purposes and does not involve potential financial gain. It is understood that any copying from, or publication of, this dissertation which involves potential financial gain will not be allowed without written permission.

for . . . . . "

A MATHEMATICAL INVESTIGATION  
OF THE OCCURRENCE OF VORTICES  
IN FLOW PAST IRREGULAR SURFACES

A THESIS

Presented to  
the Faculty of the Graduate Division  
by

Robert Desmond King

In Partial Fulfillment  
of the Requirements for the Degree  
Master of Science in Applied Mathematics

Georgia Institute of Technology  
September, 1959

A MATHEMATICAL INVESTIGATION  
OF THE OCCURRENCE OF VORTICES  
IN FLOW PAST IRREGULAR SURFACES

Approved by:

\_\_\_\_\_  
\_\_\_\_\_  
\_\_\_\_\_  
\_\_\_\_\_

Date of Approval:

26th August 1959.

## ACKNOWLEDGEMENT

I wish to thank my thesis advisor, Dr. J. N. Hunt, for suggesting this thesis topic and for his guidance during the course of this study.

## TABLE OF CONTENTS

	Page
ACKNOWLEDGEMENT. . . . .	ii
LIST OF ILLUSTRATIONS. . . . .	iv
SUMMARY. . . . .	v
Chapter	
I. CONFORMAL MAPPING . . . . .	1
The Schwarz-Christoffel Theorem	
Single Thin Obstacle Projecting from an Infinite Wall	
Infinite Row of Thin Obstacles Projecting from a Wall	
Infinite Saw-toothed Contour	
II. VORTEX MOTION AND HYDRODYNAMICAL STABILITY. . .	16
Vortex Motion	
Hydrodynamical Stability	
Stability Theorem	
III. THE OCCURRENCE OF VORTICES AND VORTEX WAKES . .	28
Two-dimensional Flow past a Flat Plate	
Stability of the Flow	
Velocity at the Edges of the Plate	
Drag Coefficient for a Flat Plate at Low Speeds	
Karman Momentum Method for High Speeds	
IV. CONCLUSIONS . . . . .	45
BIBLIOGRAPHY . . . . .	51

## LIST OF ILLUSTRATIONS

Figure	Page
1. Single Thin Obstacle Projecting from an Infinite Wall. . . . .	48
2. Infinite Row of Thin Obstacles Projecting from a Wall . . . . .	48
3. Infinite Saw-toothed Contour . . . . .	49
4. Vortex Pair in Steady Streaming. . . . .	49
5. Vortex Pair in the Presence of a Flat Plate . . . . .	50
6. Karman Vortex Street . . . . .	50

## SUMMARY

This thesis is concerned with devising methods for the mathematical investigation and construction of vortex flows past irregular surfaces and the calculation of the resulting drag coefficients. The drag experienced by a liquid flowing over a rough surface is attributable to two causes: the dissipation of energy in the viscous boundary layer and the loss of momentum in the formation of vortex trails. The first of these causes is fairly well understood; but little is known about conversion of main flow momentum into vortices, which may be stationary or may be carried downstream with the flow.

A great portion of classical hydrodynamics is concerned with conformal transformations, for the problem of devising potential flows around a body of complicated shape can often be simplified considerably by conformally mapping the complicated body onto a simpler one. Less extensive use has been made of conformal mappings for flows containing vortices. Realistic mathematical models of fluid flows, in particular flows past surfaces with jutting protuberances, must take account of the formation of vortices at all but extremely low speeds. The first section of this thesis is devoted to the derivation of functions which map complicated contours onto a topologically simpler half-plane. The

Schwarz-Christoffel mapping theorem is quoted and used to construct mapping functions of this type for several surfaces.

Stability of vortex configurations is a criterion often used to determine whether mathematically constructed flows are physically feasible, and it is useful to know how stability of vortex configurations is affected by a conformal mapping. To this end, the notion of first-order stability of a vortex arrangement is introduced, and it is proved that first-order stability is invariant under a conformal mapping.

The results so obtained are then applied to steady flow containing two vortices past a flat plate normal to the streaming, this being the simplest example of a projection from an infinitely long wall. The important investigations into this and related problems like the Karman vortex street are summarized, and the theoretical drag coefficient of the plate is calculated and compared with experimental values. This section is concluded with a discussion of the application of Euler's momentum theorem to the derivation of drag formulas for vortex streets.

In the final section of this thesis, it is indicated how the methods developed here may be applied to more general perfect fluid flows past irregular surfaces. Particular attention is paid to those flows which cause variations of the Karman vortex street.



## CHAPTER I

## CONFORMAL MAPPING

It is well-known [1] that the class of solutions of Laplace's equation

$$u_{xx} + u_{yy} = 0$$

is invariant under one-to-one conformal transformations of the complex variable  $z = x + iy$ . The importance of conformal transformations in hydrodynamics is due chiefly to this result, for potential functions representing ideal flows are solutions of Laplace's equation subject to appropriate boundary conditions. Laplace's equation is often easiest to solve for a disk or a half-plane. If a problem is stated for a region of complicated shape, a solution may be found by mapping the given region conformally onto a disk or half-plane. It is, therefore, of great importance to be able to map regions onto one another conformally.

The well-known Riemann mapping theorem guarantees that this can be done under very general conditions. An exact statement of this theorem is [2] as follows: any simply-connected schlicht domain  $D$  whose boundary consists of more than one point can be mapped conformally onto the interior of the unit circle. It is, moreover, possible to make an arbitrary point of  $D$  and direction through this point correspond,

respectively, to the origin and the direction of the positive axis. If this is done, the mapping is unique. Since the upper half-plane can be mapped conformally onto the interior of the unit circle by a linear transformation, arbitrary domains as specified in Riemann's theorem can be mapped conformally onto either a half-plane or the unit disk. The Riemann mapping theorem does not give any practical means of constructing the mapping function which achieves the desired transformation. The necessity thus arises of developing special techniques for deriving the mapping function in a given case. One of the most useful methods for transforming domains in hydrodynamics is the theorem of Schwarz and Christoffel, which gives the mapping function for a polygon onto a half-plane in terms of an integral.

The Schwarz-Christoffel theorem.--Let  $a_1, a_2, \dots, a_n$  be  $n$  points on the real axis in the  $s$ -plane such that

$$a_1 < a_2 < \dots < a_n.$$

Let  $u_1, u_2, \dots, u_n$  be interior angles of a simple closed polygon of  $n$  vertices, all in the finite plane, so that

$$u_1 + u_2 + \dots + u_n = (n-2)\pi. \quad (1)$$

Then the transformation from the  $s$ -plane to the  $z$ -plane defined by

$$\frac{dz}{ds} = K(s-a_1)^{u_1/\pi-1} \dots (s-a_n)^{u_n/\pi-1} \quad (2)$$

transforms the real axis in the  $s$ -plane into the boundary of a closed polygon in the  $z$ -plane in such a way that the vertices of the polygon correspond to the points  $a_1, a_2, \dots, a_n$  and the interior angles of the polygon are  $u_1, u_2, \dots, u_n$ . Moreover, when the polygon is simple, the interior is mapped by the transformation onto the upper half of the  $s$ -plane. The quantity  $K$  is a constant which may be complex.

A rigorous proof of the Schwarz-Christoffel theorem is given by Nehari [3] for the case in which none of the points  $a_1, a_2, \dots, a_n$  coincides with the point at infinity. This restriction can be relaxed by a simple linear transformation to allow one of the points  $a_i$  to coincide with the point at infinity. Suppose  $a_n$  is transformed into the point at infinity by the linear transformation

$$w = 1/(a_n - s),$$

or upon solving for  $s$ ,

$$s = a_n - (1/w).$$

If equation (2) is integrated, the mapping function is found to be

$$z = K \int_0^s (t-a_1)^{u_1/\pi-1} \dots (t-a_n)^{u_n/\pi-1} dt + C, \quad (3)$$

where  $C$  is a constant of integration. If the dummy variable  $t$  is replaced by means of the equation

$$t = a_n - (1/v),$$

equation (3) becomes

$$z = K \int_0^w (a_n - a_1 - \frac{1}{v})^{u_1/\pi-1} \cdot \cdot \cdot \left(-\frac{1}{v}\right)^{u_n/\pi-1} dv/v^2 + C_1. \quad (4)$$

If  $u_n$  is eliminated by means of equation (1) and if the constant  $K$  is combined with constants arising from simplification into a new constant  $K_1$ , equation (4) becomes

$$z = K_1 \int_0^w (v-b_1)^{u_1/\pi-1} \cdot \cdot \cdot (v-b_{n-1})^{u_{n-1}/\pi-1} dv + C_1,$$

where  $b_1, b_2, \dots, b_{n-1}$  are constants. Hence, the effect on equation (3) of one of the points  $a_1$  coinciding with the point at infinity consists in the corresponding point being left out of the mapping formula.

In the form of the Schwarz-Christoffel theorem given above, it is assumed that no point of the simple closed polygon to be mapped coincides with the point at infinity. However, the proof has been modified slightly by Mangler [4] to include the case in which one or more of the vertices of the polygon are infinitely distant. In this representation an infinite parallel strip may be thought of as a rectangle with its four corners at infinity. The "interior angle" of a corner at infinity has zero radian measure. Mangler also proved the theorem for the case in which two sides of the polygon coincide. Use will be made of these extensions in

the following examples.

Single thin obstacle projecting from an infinite wall.--It requires only a simple application of the Schwarz-Christoffel theorem to map the lower half of the  $z$ -plane with a single obstacle projecting normally from it onto the lower half of the  $s$ -plane. This configuration is shown in Fig. 1. This mapping will be used later to construct a fluid flow past such a boundary.

In order to apply the Schwarz-Christoffel theorem, the configuration in the  $z$ -plane must be considered a polygon with three vertices in the finite plane [one at  $(0,L)$ , two at  $(0,0)$ ] and one at infinity. Two sides of the polygon are coincident--namely, the side extending from  $(0,0)$  to  $(0,L)$  on the imaginary axis and the side from  $(0,L)$  to  $(0,0)$ . This polygon is now to be mapped onto the  $s$ -plane so that the vertex at  $(0,L)$  goes into  $(0,0)$ , one vertex at  $(0,0)$  goes into  $(a,0)$ , the other at  $(0,0)$  goes into  $(-a,0)$ , and the half-plane  $\text{Im}(z) \leq 0$  goes onto  $\text{Im}(s) \leq 0$ . [  $\text{Im}(z)$  denotes the imaginary part of  $z$ . ] The vertex at infinity in the  $z$ -plane is mapped into the point at infinity in the  $s$ -plane; hence, as was shown earlier, this term does not appear in the mapping formula. The angle at the two vertices at  $(0,0)$  in the  $z$ -plane contains  $\pi/2$  radians measured counterclockwise, and the angle at  $(0,L)$  contains  $2\pi$  radians. By equation (2), with  $u_1 = u_3 = \pi/2$ ,  $u_2 = 2\pi$ ,  $a_1 = a$ ,  $a_2 = 0$ , and  $a_3 = -a$ , the mapping formula is

$$\frac{dz}{ds} = K(s-a)^{-\frac{1}{2}}(s-0)(s+a)^{-\frac{1}{2}} = Ks/(s^2-a^2)^{\frac{1}{2}}.$$

Integration of this equation yields

$$z = K\sqrt{s^2-a^2} + C.$$

Since  $z = iL$  when  $s = 0$  and  $z = 0$  when  $s = \pm a$ ,  $C = 0$  and  $K = L/a$ . The constant  $a$  may be chosen arbitrarily; a convenient choice for  $a$  is  $L$ --the height of the projection. These substitutions yield

$$z = \sqrt{s^2-L^2} \quad (5)$$

as the desired mapping function. The mapping from the  $z$ -plane to the  $s$ -plane is given by

$$s = \pm\sqrt{z^2+L^2},$$

where the plus or minus sign is chosen depending on which part of the  $s$ -plane is being investigated.

It should be noticed that this mapping is conformal at all points of the polygon except the vertices. This is a general feature of mapping functions obtained by the Schwarz-Christoffel theorem, as equation (2) shows.

Infinite row of thin obstacles projecting from a wall.--The next case to be considered is the arrangement shown in Fig. 2: an infinite row of equally spaced thin obstacles of the same length projects normally from a wall. This situation may be regarded as an idealized model of a sandy ocean

bottom under the action of simple harmonic waves. The sand tends to build up in crests and troughs, and vortices are shed by a fluid streaming steadily or periodically over the bottom. Similarly, such a model may be used to represent almost any hydraulically rough surface. An extension to the representation of radially symmetric flow within a rough pipe may be visualized. It will be indicated later in this thesis how this mapping can be used to construct a fluid flow over such a surface.

Strictly speaking, the Schwarz-Christoffel theorem cannot be applied to this configuration; for the polygon has an infinite number of vertices, and the Schwarz-Christoffel theorem was proved for a finite number. However, by proceeding as though the theorem did apply, a mapping function may be constructed. Then it must be shown that the function so found does, indeed, effect the desired transformation.

Suppose the  $z$ -plane is mapped onto the  $s$ -plane in such a way that the vertex at  $(0,L)$  goes into  $(0,0)$ , the vertices at  $(0,0)$  go into  $(a,0)$  and  $(-a,0)$ , the vertex at  $(d,L)$  goes into  $(2a+b,0)$ , those at  $(d,0)$  go into  $(a+b,0)$  and  $(3a+b,0)$ , and so on. Equation (2) becomes

$$\frac{dz}{ds} = K \left[ (s-a)^{-\frac{1}{2}} s (s+a)^{-\frac{1}{2}} \right] \left[ \left( s-(a+b) \right)^{-\frac{1}{2}} \left( s-(2a+b) \right) \left( s-(3a+b) \right)^{-\frac{1}{2}} \right] \quad (6)$$

$$\cdot \cdot \cdot \left[ \left( s+(a+b) \right)^{-\frac{1}{2}} \left( s+(2a+b) \right) \left( s+(3a+b) \right)^{-\frac{1}{2}} \right] \cdot \cdot \cdot$$

Now upon rearrangement of terms and introduction of the

product notation

$$\prod_{n=1}^{\infty} A_n = A_1 A_2 \dots,$$

equation (6) becomes

$$\frac{dz}{ds} = K \frac{s \prod_{n=1}^{\infty} [s^2 - n^2(2a+b)^2]}{\left[ \prod_{n=0}^{\infty} (s^2 - [(2n-1)a + nb]^2) \prod_{n=1}^{\infty} (s^2 - [(2n+1)a + nb]^2) \right]^{\frac{1}{2}}} \cdot (7)$$

For convenience let

$$A = a + b$$

and

$$B = 2a + b.$$

Then rearrangement of the denominator of expression (7) leads to

$$\frac{dz}{ds} = K \frac{s \prod_{n=1}^{\infty} (s^2 - n^2 B^2)}{\left\{ \left( (s-A) \prod_{n=1}^{\infty} [(s-A)^2 - n^2 B^2] \right) \left( (s+A) \prod_{n=1}^{\infty} [(s+A)^2 - n^2 B^2] \right) \right\}^{\frac{1}{2}}} \cdot (8)$$

Now  $\sin(z)$  can be expressed [5] as an infinite product in the form

$$\sin(z) = z(1 - z^2/\pi^2)(1 - z^2/2^2\pi^2) \dots$$

The infinite products in equation (8) can be rewritten as



$$\frac{dz}{ds} = \frac{K_1 \frac{\pi s}{B} \prod_{n=1}^{\infty} \left[ 1 - \frac{s^2}{n^2 B^2} \right]}{\left[ \left( \frac{\pi(s-A)}{B} \prod_{n=1}^{\infty} \left[ 1 - \frac{(s-A)^2}{n^2 B^2} \right] \right) \left( \frac{\pi(s+A)}{B} \prod_{n=1}^{\infty} \left[ 1 - \frac{(s+A)^2}{n^2 B^2} \right] \right) \right]^{\frac{1}{2}}},$$

where the constants arising through rearrangement of terms are combined with  $K$  to form a new constant  $K_1$ . In view of the product representation of the sine, this last result may be written

$$\frac{dz}{ds} = \frac{K_1 \sin(\pi s/B)}{\left[ \sin \frac{\pi(s-A)}{B} \cdot \sin \frac{\pi(s+A)}{B} \right]^{\frac{1}{2}}} \quad (9)$$

Equation (9) may be reduced by means of the trigonometric identities

$$2\sin(x+y)\sin(x-y) = \cos(2y) - \cos(2x)$$

and

$$\cos(2x) = 2\cos^2(x) - 1$$

to the equation

$$\frac{dz}{ds} = \frac{K_1 \sin(\pi s/B)}{\left[ 1 + \cos(2\pi A/B) - 2\cos^2(\pi s/B) \right]^{\frac{1}{2}}} \quad (10)$$

Equation (10) can be integrated to give the mapping function

$$\cos[(z-c)/k] = \frac{\cos[\pi s/(2a+b)]}{\cos[(a+b)\pi/(2a+b)]} \quad (11)$$

where  $c$  is a constant of integration and  $k$  is the constant in the Schwarz-Christoffel theorem.

Since the Schwarz-Christoffel theorem did not apply in this case, it has to be proved directly that the mapping function given by equation (11) achieves the desired transformation. It must be the case in hydrodynamical applications that parts of the  $s$ -plane and the  $z$ -plane far removed from the obstructions correspond unaltered, since a uniform stream at infinity in the  $z$ -plane should correspond to a uniform stream in the  $s$ -plane. It suffices to show that

$$dz/ds \rightarrow \text{constant as } \text{Im}(s) \rightarrow +\infty .$$

Replace  $s$  in equation (10) by the quantity  $it$ , where  $t$  is real. Since

$$\sin(it) = i \sinh(t)$$

and

$$\cos(it) = \cosh(t);$$

equation (10) becomes

$$\frac{dz}{ds} = K_1 i \left[ \frac{1 + \cosh(2\pi A/B)}{\sinh^2(\pi t/B)} - 2\coth^2(\pi t/B) \right]^{-\frac{1}{2}} .$$

Now

$$\sinh(\pi t/B) \rightarrow +\infty$$

and

$$\coth(\pi t/B) \rightarrow 1$$

as  $t \rightarrow +\infty$  , so that

$$dz/ds \rightarrow K_1 i(-2)^{-\frac{1}{2}} = \text{constant}$$

as

$$t = \text{Im}(s) \rightarrow +\infty .$$

Therefore, distant parts of the two planes correspond unaltered save for a constant multiplicative factor.

Next, it must be shown that the mapping function has periodic singularities corresponding to the points

$$iL, \pm d+iL, \pm 2d+iL, \dots$$

in the  $z$ -plane, which are the vertices of the polygon. The constant  $c$  in equation (11) causes a translation of axes; it may, therefore, be taken equal to zero without affecting the character of the mapping.

In order to relate  $k$  to the given parameter  $L$ , suppose that  $z = iL$  is mapped into  $s = 0$ . Then

$$\cos(iL/k) = \frac{1}{\cos \frac{a+b}{2a+b} \pi}, \quad (12)$$

or

$$L = -ik \cos^{-1} \left\{ \frac{1}{\cos \frac{a+b}{2a+b} \pi} \right\} .$$

This gives  $L$  in terms of  $k$ , where the principal value of the complex inverse cosine is to be chosen. From equation (12)

$$\sin(iL/k) = i \tan \frac{a+b}{2a+b} \pi . \quad (13)$$

Suppose that

$$s = (2a+b)n, \quad n = \pm 1, \pm 2, \dots$$

These are the points in the  $s$ -plane into which the vertices of the polygon in the  $z$ -plane are mapped. Suppose that

$$z = p + iL.$$

Then equation (11) becomes

$$\cos(p/k + iL/k) = \frac{(-1)^n}{\cos \frac{a+b}{2a+b} \pi} . \quad (14)$$

The left side of this equation may be expanded by the formula

$$\cos(x+y) = \cos(x)\cos(y) - \sin(x)\sin(y) .$$

If this is done and the substitutions indicated in equations (12) and (13) are made, equation (14) reduces to

$$(-1)^n = \cos(p/k) - i \sin(p/k) \sin \frac{a+b}{2a+b} \pi .$$

This implies that

$$p = n\pi k .$$

The mapping is thus periodic in  $z$  with period  $\pi k$ , and the constants  $a$ ,  $b$ ,  $c$ , and  $k$  in the mapping function (11) may be adjusted to give singularities at the points corresponding to

$$z = iL + nd, \quad n = 0, \pm 1, \pm 2, \dots .$$

The preceding argument shows that the mapping function (11) transforms the domain in Fig. 2 onto the lower half of the  $s$ -plane. This domain was a polygon with an infinite number of vertices, and the proof of the Schwarz-Christoffel theorem did not apply for such polygons. Yet in this case it was possible to show directly that the mapping function obtained by formal application of the Schwarz-Christoffel theorem did actually perform the desired transformation.

Infinite saw-toothed contour.---The last mapping to be considered is the infinite serrated contour pictured in Fig. 3. Designate by  $\phi$  the acute angle of each tooth, all of the teeth being equal in size and similar in shape. The surface extends infinitely far to the right and left. This polygon, like the last one, may be considered a model of a hydraulically rough surface.

The application of the Schwarz-Christoffel theorem

to this polygon follows in all major points the procedure for the last polygon. Suppose that the vertices are mapped into the points

$$(\pm a, 0), (\pm 2a, 0), \dots$$

of the  $s$ -plane. Substitution into equation (2) yields an infinite product, which may be reduced by means of the formulas [5]

$$\sin(z) = z(1 - z^2/\pi^2)(1 - z^2/2^2\pi^2) \dots$$

and

$$\cos(z) = (1 - 4z^2/\pi^2)(1 - 4z^2/3^2\pi^2) \dots$$

to the equation

$$dz/ds = K \left[ \cot(\pi s/2a) \right]^{1-\phi/\pi}.$$

This can be integrated in the special case  $\phi = \pi/2$  by letting

$$u = \left[ \cot(\pi s/2a) \right]^{\frac{1}{2}}.$$

This yields

$$z = K_1 \int \frac{u^2}{1+u^4} du,$$

or

$$z = K_2 \left[ \log \frac{u^2 + u\sqrt{2+1}}{u^2 - u\sqrt{2+1}} - 2 \tan^{-1} \frac{u\sqrt{2}}{1-u^2} \right] + c .$$

The function  $z$  is given explicitly in terms of  $s$  upon replacement of  $u$  by

$$\left[ \cot(\pi s/2a) \right]^{\frac{1}{2}} .$$

It should be emphasized again that the proof of the Schwarz-Christoffel theorem did not apply for a polygon of the sort dealt with above, which has an infinite number of vertices. It must be shown directly that the mapping derived above does actually map the polygon in Fig. 3 onto the half-plane. The details of this proof will be omitted since the procedure is the same as in the verification of the previous mapping function.

## CHAPTER II

## VORTEX MOTION AND HYDRODYNAMICAL STABILITY

Vortex motion.--The fluid considered in the remainder of this thesis is non-viscous and incompressible, so that the velocity components  $u$  and  $v$  satisfy the equation of continuity

$$u_x + v_y = 0 .$$

The fluid motion is irrotational except for isolated rectilinear vortices, a fact which implies the existence of a velocity potential satisfying Laplace's equation. The complex potential for a vortex at the point  $z_0$  may be written [6]

$$w = ik \log(z-z_0) .$$

The quantity  $k$  is called the strength of the vortex. The circulation is defined as

$$\int_C u dx + v dy ,$$

where  $C$  is a simple closed curve around  $z_0$ . The circulation about a single vortex is therefore  $2\pi k$ .

In general, if  $w = f(z)$  is the complex potential of a flow,  $f(z)$  will be assumed analytic throughout the entire



$z$ -plane except, perhaps, for isolated poles. The velocity components  $u$  and  $v$  of the flow are related to the potential function by the equation

$$-u + iv = dw/dz$$

at all points where  $w(z)$  is analytic.

A vortex possesses no tendency to set itself in motion [7]. Hence, the velocity of a vortex at a point  $P$  is compounded of the velocity induced by other vortices and by the general velocity at  $P$  of the fluid due to the remaining causes (sources, sinks, etc.). Thus, if  $w(z)$  is the complex potential of a flow which contains a vortex of strength  $k$  at the point  $z_0$ , the complex velocity of the vortex is

$$-u_0 + iv_0 = \frac{d}{dz} \left[ w(z) - ik \log(z - z_0) \right]_{z = z_0}. \quad (15)$$

Hydrodynamical stability.--The stability of any dynamical system is generally investigated in the following manner: the system is displaced slightly from its equilibrium position, and all but first-order terms of the original displacement are neglected in the equations of motion. If the initial disturbance is found to grow exponentially with time, the system is unstable. If the initial displacement is damped out, if it is periodic, or if it grows linearly with time, the system is described as being stable. More precisely, the system is said to have first-order stability.

This is essentially the definition adopted by Birkhoff and Zarantonello [8] and by Rosenhead [9].

Stability is an important criterion for determining whether a theoretical fluid flow can actually exist in nature. If a flow containing vortices is mathematically constructed and then found to be unstable, this means that such a flow can exist in reality only for a very short time, if at all.

Conformal mappings are frequently used to construct fluid flows. If a hydrodynamical configuration is stable in one plane and if the variable is subjected to a conformal mapping, then there is no particular reason for supposing that the new configuration is either stable or unstable. That first-order stability (or instability) is preserved under a conformal transformation of the variable is proved by the theorem established in the next section.

Stability theorem.--First-order stability of a stationary hydrodynamical system subjected to small translatory disturbances is preserved under a conformal mapping.

Proof: Let  $w(s)$  be the complex potential function for a flow containing a vortex (the theorem is equally valid for sources or sinks). Let

$$w_1(s) = w(s) - ik \log(s-s_0),$$

where  $w_1(s)$  is analytic at  $s = s_0$ . By equation (15),

$$\left. \frac{dw_1}{ds} \right]_{s=s_0}$$

gives the complex velocity of the singularity at  $s_0$ . The logarithmic part of  $w_1(s)$  represents a vortex if  $k$  is real, a source or sink if  $k$  is imaginary, and a spiral flow if  $k$  is complex. In what follows,  $k$  is supposed to be real, although this condition is not necessary for the validity of the proof. Suppose the vortex is at rest at the point

$$s_0 = c_0 + id_0$$

in the  $s$ -plane. If

$$s = x + iy$$

and

$$w_1'(s) = -u(x,y) + iv(x,y) , \quad (16)$$

then

$$\begin{cases} u(c_0, d_0) = 0 \\ v(c_0, d_0) = 0 \end{cases} , \quad (17)$$

where  $u$  and  $v$  are velocity components of the vortex at  $s_0$ . The stability of a stagnation point is thus also included in the proof by taking the limit as  $k \rightarrow 0$ .

Suppose that  $s$  is subjected to a conformal mapping  $z = z(s)$ . Let

$$z'(s) = H(s) = F(x,y) + iG(x,y) .$$

Since the mapping is conformal,

$$dz/ds \neq 0$$

at  $(c_0, d_0)$ . Suppose that  $w(s)$  is transformed into  $W(z)$  by this mapping. It is known [10] that vortices transform into vortices under conformal transformations. Therefore,

$$W_1(z) = W(z) - ik \log[s(z) - s_0],$$

where  $s(z)$  is the inverse of  $z = z(s)$ , represents the velocity potential at

$$z_0 = z(s_0)$$

of a flow containing a vortex at  $z_0$ . By the rule for differentiating functions implicitly,

$$w_1'(s) = W_1'(z) \frac{dz}{ds}. \quad (18)$$

But since

$$\left. \frac{dz}{ds} \right|_{s_0} \neq 0$$

due to the conformality of the mapping, the vortex will be at rest in the  $z$ -plane at the point  $z_0$  corresponding to  $s_0$  under  $z = z(s)$ .

If  $U$  and  $V$  are the velocity components of the vortex at  $z_0$ , then

$$-U + iV = \frac{dw_1/ds}{dz/ds} = \frac{-u(x,y) + iv(x,y)}{F(x,y) + iG(x,y)}. \quad (19)$$

Equation (19) can be separated into real and imaginary parts to yield

$$U = \frac{Fu - Gv}{|H|^2} \quad (20)$$

and

$$V = \frac{Fv + Gu}{|H|^2} . \quad (21)$$

To determine how stability is affected by a conformal transformation, stability conditions in the  $s$ -plane will first be derived. Suppose that the vortex at rest at the point

$$s_0 = c_0 + id_0$$

is displaced slightly to the point

$$s_0 + \delta s = (c_0 + id_0) + (a + ib),$$

where  $|\delta s|$ ,  $|a|$ , and  $|b|$  are small. The quantities  $a$  and  $b$  must not grow exponentially with increasing time if the vortex at  $s_0 + \delta s$  is stable. Then the potential function for the vortex at  $s_0 + \delta s$  is

$$w_1(s) = w(s) - ik \log[s - (s_0 + \delta s)] ,$$

where  $w(s)$  is the potential function for the flow with the vortex displaced to  $s_0 + \delta s$ . Then from equation (16),

$$w_1'(s_0 + \delta s) = -u(c_0 + a, d_0 + b) + iv(c_0 + a, d_0 + b) .$$

The functions  $u(x,y)$  and  $v(x,y)$  are assumed to have partial derivatives of all orders at  $(c_0, d_0)$ , so that both functions may be expanded in a Taylor's series about that point.

First-order stability is presently being investigated; therefore, powers of  $a$  and  $b$  higher than the first will be neglected in the expansion. The last equation then becomes

$$dw/ds = -u(c_0, d_0) - au_x - bu_y + i[v(c_0, d_0) + av_x + bv_y], \quad (22)$$

where all partial derivatives are to be evaluated at the point  $(c_0, d_0)$ . By equation (17),  $u$  and  $v$  evaluated at  $(c_0, d_0)$  are zero. If

$$-da/dt + idb/dt = w_1'(s_0 + \delta s),$$

then equation (22) may be separated into real and imaginary parts to give

$$\begin{cases} da/dt = (u_x)a + (u_y)b \\ db/dt = (v_x)a + (v_y)b, \end{cases} \quad (23)$$

where  $t$  represents time. All partial derivatives will be evaluated at  $(c_0, d_0)$  in the remainder of this proof unless the contrary is specified. Let

$$A = u_x, B = u_y, X = v_x, Y = v_y .$$

The fluid is assumed incompressible; hence, the equation of

continuity

$$u_x + v_y = 0$$

is satisfied, or  $A = -Y$ . Under these conditions, the differential equations (23) of stability become

$$\begin{cases} da/dt = Aa + Bb \\ db/dt = Xa + Yb \end{cases} \quad (24)$$

This system of equations can be combined to give the single differential equation

$$d^2a/dt^2 = (BX - AY)a .$$

This equation has the general solution

$$a = c_1 e^{rt} + c_2 e^{-rt} ,$$

where

$$r = \sqrt{BX - AY} .$$

For stability,  $a$  must not grow exponentially; that is,  $r$  must not be both real and different from zero. This implies that  $r$  must be either zero or imaginary, which means that  $BX - AY$  must be zero or negative. The preceding argument has led to the following stability conditions: the system is stable if  $BX - AY \leq 0$ ; it is unstable if  $BX - AY > 0$ .

It now remains to investigate the stability in the

$z$ -plane. The transformation  $z = z(s)$  maps  $s_0$  into  $z_0$ . It was shown above that the vortex is at rest at  $z_0$ . Displace this vortex to the point  $z_0 + \delta z$ , where  $|\delta z|$  is small. This displacement corresponds to some perturbation in the  $s$ -plane, say  $\delta s$ . But since

$$dz/ds = H(s),$$

$\delta z$  and  $\delta s$  are related by the equation

$$\delta z = H(s) \delta s$$

to a first-order approximation. Let

$$z = m + in$$

and

$$s = a + ib.$$

Since

$$H(s) = F(x, y) + iG(x, y),$$

the perturbations in the two planes are related by

$$m + in = (F + iG)(a + ib),$$

where for convenience the arguments  $x$  and  $y$  in the functions  $F$  and  $G$  have been omitted. This last equation can be separated into real and imaginary parts to yield

$$m = Fa - Gb$$



and

$$n = Ga + Fb.$$

These equations may be solved for a and b to give

$$a = \frac{Fm + Gn}{|H|^2} \quad (25)$$

and

$$b = \frac{-Gm + Fn}{|H|^2}. \quad (26)$$

From equation (20),

$$\frac{dm}{dt} = \frac{F(c_0+a, d_0+b)u(c_0+a, d_0+b) - G(c_0+a, d_0+b)v(c_0+a, d_0+b)}{[F(c_0+a, d_0+b)]^2 + [G(c_0+a, d_0+b)]^2}.$$

By assumption the functions F, G, u, and v have all orders of partial derivatives, and they may be expanded in a Taylor's series about the point  $(c_0, d_0)$ . If higher-order terms in a and b are neglected, the last equation becomes

$$\frac{dm}{dt} = \frac{[Fu_x - Gv_x]a + [Fu_y - Gv_y]b}{|H|^2}.$$

By a similar calculation using equation (21),

$$\frac{dn}{dt} = \frac{[Fv_x + Gu_x]a + [Fv_y + Gu_y]b}{|H|^2}.$$

The quantities  $a$  and  $b$  can be eliminated from these two equations by means of equations (25) and (26). This gives the two equations of stability in the  $z$ -plane

$$\begin{cases} dm/dt = A^* m + B^* n \\ dn/dt = X^* m + Y^* n, \end{cases} \quad (27)$$

where

$$A^* = \frac{F^2 A + G^2 Y - FG(B+X)}{|H|^2}, \quad (28)$$

$$B^* = \frac{F^2 B - G^2 X + FG(A-Y)}{|H|^2},$$

$$X^* = \frac{F^2 X - G^2 B + FG(A-Y)}{|H|^2},$$

$$A^* = -Y^*.$$

Equations (27) have the same form as the stability equations (24) in the  $s$ -plane. The system represented by equations (27) is, therefore, stable if

$$B^* X^* - A^* Y^* \leq 0.$$

Direct calculation from equations (28) reveals after reduction that

$$B^* X^* - A^* Y^* = (BX - AY)/|H|^4.$$

Since  $|H|^4$  is always positive (it cannot be zero because the mapping is conformal), the sign of  $B^* X^* - A^* Y^*$  is the same

as the sign of  $BX - AY$ . But the sign of these quantities is the criterion which determines whether the system is stable or unstable. Therefore, stability (or instability) in one plane implies stability (or instability) in the other plane, and first-order stability is preserved under a conformal mapping.

It will be indicated in the last section of this thesis how the preceding stability theorem can be applied to special flows. In general, one can profitably use this theorem in the following way: suppose flow past an irregular surface is obtained by conformally mapping a vortex configuration onto the irregular surface. Stability calculations, which can be quite involved algebraically, are usually easiest to carry through for the vortex arrangement in the absence of the irregular surface. If a calculation reveals that the simpler configuration is stable, then the more complicated vortex configuration caused by flow past the surface will also be stable, as the preceding theorem demonstrated. Hence, it is not necessary to carry through the more complicated stability calculation for flow past the irregular surface.

## CHAPTER III

## THE OCCURRENCE OF VORTICES AND VORTEX WAKES

It is frequently observed that a body moving through a fluid at low and medium Reynolds numbers produces a number of eddies in its wake. This phenomenon has been the object of many theoretical investigations since 1900.

One of the first investigators in this field was Ludwig Föppl [11], who studied the formation of a vortex pair symmetrically situated behind a moving cylinder. He concluded that the vortex pair is at rest relative to the cylinder provided it lies on a curve whose formula was stated. He also showed that any position of relative equilibrium was stable for disturbances symmetrical with respect to the axis of the wake and unstable for anti-symmetrical ones [12]. The vortices will eventually, therefore, move downstream in an unsymmetrical manner as the Reynolds number is increased.

The most significant investigation into vortex motion was that of Karman [13], who in a series of papers studied the formation of the so-called "vortex streets." He observed that the vortices tend to assume a regular pattern a distance of four to five diameters behind the cylinder. The vortices arrange themselves in a double row, in which each vortex is opposite the mid-point of the

interval between two vortices in the opposite row. Karman investigated first the case of a symmetrical double row of vortices, in which one row is the mirror-image reflection of the other in the axis of the wake. This arrangement he found to be unstable. He discovered, however, that the alternating street of vortices is stable under a periodic disturbance, provided the spacing ratio of the width of the street to the distance between vortices in the same row is a certain constant.

Karman's investigation was directed toward determining the theoretical drag associated with the double row of vortices. By application of Euler's momentum theorem to the infinite street, he derived a formula for the average drag, which gave close agreement [14] with experimental values for a cylinder and satisfactory agreement for a flat plate.

Schmieden [15] found that the Karman vortex street has second-order instability, which may account for the break-up of the vortex street after it has travelled a comparatively short distance. Rosenhead [16] studied the effect of the proximity of channel walls.

The purpose of this thesis is to devise methods for applying conformal mappings to vortex configurations like the Karman street of vortices. For example, fluid streaming over an infinite row of thin projections (see Fig. 2) produces some arrangement of vortices, which can be studied by means of the mapping function derived for that surface. The

next section deals with detailed application of the method of conformal mappings to flow past a simple surface.

Two-dimensional flow past a flat plate.--Consider the case of streaming past a single projection from an infinite wall (see Fig. 1). Suppose a vortex of strength  $-k$  is situated at the point  $a+ib$  in the first quadrant of the  $s$ -plane. In order to write down the complex potential for this vortex by the method of images, a second vortex of strength  $+k$  must be placed at the image point  $a-ib$ . The situation in the  $s$ -plane, together with a few streamlines, is shown in Fig. 4.

Impose a steady streaming of velocity  $k/2b$  in the positive direction of the real  $s$ -axis to bring the vortices to rest. The complex potential function for this flow is

$$w = -(k/2b)s + ik \log \frac{s-(a-ib)}{s-(a+ib)} . \quad (29)$$

By equation (15), the complex velocity of the vortex at  $a+ib$  is given by

$$\begin{aligned} & \frac{d}{ds} \left[ w + ik \log [s-(a+ib)] \right]_{s=a+ib} \\ &= \left[ -(k/2b) + \frac{ik}{s-(a-ib)} \right]_{s=a+ib} = 0 . \end{aligned}$$

Therefore, a steady streaming of velocity  $k/2b$  does, indeed, bring the vortex at  $a+ib$  to rest.

The mapping function

$$s = (z^2 + L^2)^{\frac{1}{2}},$$

obtained by solving equation (5) for  $s$ , may be used to construct the potential function for streaming in the presence of the vortex past the obstacle of length  $L$  in Fig. 1. If  $s$  is replaced in equation (29) by  $(z^2 + L^2)^{\frac{1}{2}}$ , this potential function is found to be

$$w = -\frac{k}{2b}(z^2 + L^2)^{\frac{1}{2}} + ik \log \frac{(z^2 + L^2)^{\frac{1}{2}} - (a - ib)}{(z^2 + L^2)^{\frac{1}{2}} - (a + ib)}. \quad (30)$$

This potential, which represents the flow shown in Fig. 5, may be thought of as describing flow containing one vortex past an obstacle protruding normally from an infinite wall, or it may alternatively be thought of as representing flow past a flat plate of length  $2L$  with a symmetrically placed pair of vortices.

Stability of the flow.—The first property of this flow to be investigated is its stability. It was shown in the course of the proof of the stability theorem that a vortex at rest in one plane remains at rest under a conformal mapping. Thus, the vortex is at rest in the  $z$ -plane at the point

$$z_0 = \sqrt{(a + ib)^2 - L^2}. \quad (31)$$

It can easily be shown that the pair of vortices has

first-order stability under symmetrical disturbances in the  $s$ -plane, a fact which implies according to the stability theorem that the pair in the  $z$ -plane also has first-order stability. In this case, however, it is not difficult to show directly the first-order stability in the  $z$ -plane.

From equation (31),

$$a-ib = (\bar{z}_0^2 + L^2)^{\frac{1}{2}},$$

where  $\bar{z}_0$  denotes the complex conjugate of  $z_0$ . Then equation (30) becomes

$$w = -\frac{k(z^2+L^2)^{\frac{1}{2}}}{2b} + ik \log \frac{(z^2+L^2)^{\frac{1}{2}} - (\bar{z}_0^2+L^2)^{\frac{1}{2}}}{(z^2+L^2)^{\frac{1}{2}} - (z_0^2+L^2)^{\frac{1}{2}}}. \quad (32)$$

Suppose the vortices at  $z_0$  and  $\bar{z}_0$  are displaced, respectively, to  $z_0 + \delta z$  and  $\bar{z}_0 + \delta \bar{z}$ . This represents a symmetrical disturbance with respect to the real  $z$ -axis. The complex velocity of the displaced vortex at  $z_0 + \delta z$  is

$$w'(z_0 + \delta z) = \frac{z}{(z^2+L^2)^{\frac{1}{2}}} \left\{ \frac{ik}{(z^2+L^2)^{\frac{1}{2}} - (\bar{z}^2+L^2)^{\frac{1}{2}}} - (k/2b) \right\},$$

where

$$z = z_0 + \delta z.$$

Now expand all quantities by the binomial theorem, neglecting powers of  $\delta z$  higher than the first. Since



$$\left. dw/dz \right]_{z_0} = 0 ,$$

the complex velocity can be simplified to the form

$$dw/dz = \frac{z_0}{a+ib} (k/4b^2) \left[ \frac{z_0 \delta z}{a+ib} - \frac{\bar{z}_0 \delta \bar{z}}{a-ib} \right] . \quad (33)$$

Let

$$\delta z = m+in . \quad (34)$$

If  $z_0$  and  $\delta z$  are eliminated from equation (33) by means of equations (31) and (34) and if

$$dw/dz = -dm/dt + i dn/dt ,$$

then the real and imaginary parts of equation (33) can be separated to give

$$\begin{cases} dm/dt = -K[Bm + (A+C)n] \\ dn/dt = -K[(A-C)m - Bn] \end{cases} \quad (35)$$

as the two equations of stability. Here,

$$K = (k/4b^2)(a^2+b^2),$$

$$A = (a^2+b^2) - L^2(a^2-b^2),$$

$$B = 2abL^2,$$

$$C = (a^2+b^2) \left[ (a^2+b^2)^2 + L^4 - 2L^2(a^2-b^2) \right]^{\frac{1}{2}} .$$

Equations (35) may be combined to give the single stability

equation

$$d^2m/dt^2 = K^2(A^2 - C^2 + B^2)m . \quad (36)$$

Upon direct substitution of the values of K, A, B, and C given above into equation (36), one finds that

$$A^2 - C^2 + B^2 = 0 .$$

Therefore, the stability equation (36) becomes

$$d^2m/dt^2 = 0 ,$$

which has the general solution

$$m = c_1 t + c_2 .$$

The disturbance grows therefore, at most, linearly with time, which is classified as stable behavior (an unstable system is one in which an initial disturbance grows exponentially). This linear growth of a symmetric perturbation may explain why the vortex trails behind flat plates do not have so clear and definite a pattern as vortices behind a cylinder [17], for which a stability calculation shows that symmetric disturbances cause an oscillation about the equilibrium position [12].

Velocity at the edges of the plate.--It must be the case in a physically real flow that the fluid velocity at the ends of the plate is finite. In potential streaming past a plate in the absence of vortices, the velocity at the ends

is infinite, which is one reason why potential flows are in some details rather poor models of real flows.

The flow presently being investigated has a finite velocity at the edges when

$$a = \sqrt{3} b ;$$

that is, the vortex must lie on the curve which is the mapping under

$$z = (s^2 - L^2)^{\frac{1}{2}}$$

of the line

$$y = (1/\sqrt{3})x,$$

where

$$s = x + iy .$$

For if

$$a = \sqrt{3} b ,$$

the complex velocity at the end of the plate is found from equation (30) to be

$$w'(iL) = \lim_{z \rightarrow iL} \frac{z}{(z^2 + L^2)^{\frac{1}{2}}} \left\{ -k/2b + ik \left[ \frac{1}{(z^2 + L^2)^{\frac{1}{2}} - (\sqrt{3} - i)b} - \frac{1}{(z^2 + L^2)^{\frac{1}{2}} - (\sqrt{3} + i)b} \right] \right\}$$

$$= \sqrt{3} \, kLi/4b^2 .$$

The x and y components of velocity at the upper end of the plate are then

$$\begin{cases} u = 0 \\ v = \sqrt{3} \, kL/4b^2 . \end{cases}$$

By symmetry the components of velocity at the lower end of the plate are

$$\begin{cases} u = 0 \\ v = -\sqrt{3} \, kL/4b^2 . \end{cases}$$

Drag coefficient for a flat plate at low speeds.--The final calculation to be made for this flow is that of the drag--the force component in the direction of the streaming. This is found by integrating the pressure over the surface exposed to the fluid. By Bernouilli's theorem the pressure p is

$$p = C - \frac{1}{2} \rho q^2 ,$$

where C is a constant,  $\rho$  is the fluid density, and q is the magnitude of the velocity. The constant C will vanish when p is integrated along both sides of the plate, so that the pressure may be taken as  $-\frac{1}{2} \rho q^2$  .

Now

$$q = \left| dw/dz \right|$$

and

$$dw/dz = (dw/ds)(ds/dz) .$$

From equation (29),

$$dw/dz = \frac{(s^2 - L^2)^{\frac{1}{2}}}{s} \left\{ -k/2b + ik \left[ \frac{1}{s - (a - ib)} - \frac{1}{s - (a + ib)} \right] \right\} . \quad (37)$$

The streamlines are symmetric about the real  $z$ -axis; hence, the total drag is twice the drag on the segment from  $z=0$  to  $z=iL$ . The variable  $s$  lies in the range

$$-L \leq s \leq +L$$

for this interval of  $z$ ; therefore,  $s$  is purely real. Let  $s=t$  to emphasize this fact.

The square of the magnitude of a complex number is equal to the product of the number and its conjugate. Therefore,

$$q^2 = |dw/dz|^2 = (dw/dz)(d\bar{w}/d\bar{z}) .$$

From equation (37),

$$q^2 = k^2 \frac{t^2 - L^2}{t^2} \left\{ 1/4b^2 - \frac{2}{[t - (a - ib)][t - (a + ib)]} + \frac{4b^2}{[t - (a - ib)]^2 [t - (a + ib)]^2} \right\} . \quad (38)$$

Since

$$z^2 = s^2 - L^2 ,$$

$zdz = sds$ . For  $z=iy$ ,  $s=t$ , and  $zdz = -ydy$ . Also,

$$-y^2 = s^2 - L^2$$

or

$$y = (L^2 - s^2)^{\frac{1}{2}} .$$

Therefore,

$$dy = -sds/(L^2 - s^2)^{\frac{1}{2}} = -tdt/(L^2 - t^2)^{\frac{1}{2}} . \quad (39)$$

The component  $dX$  of the drag is given by

$$dX = p dy ,$$

where  $p$  is the pressure. By Bernouilli's theorem,

$$dX = -\frac{1}{2}\rho q^2 dy .$$

If the substitutions indicated in equations (38) and (39) are made and if  $a$  is set equal to  $\sqrt{3} b$ , the drag increment is found to be

$$dX = \rho (3k^2/8a^2) t (L^2 - t^2)^{\frac{1}{2}} \frac{(t-2a)^2}{[t^2 - 2at + (4/3)a^2]^2} dt. \quad (40)$$

The drag on the half-plate from  $z=0$  to  $z=iL$  is the difference of the absolute magnitudes of the drag on each side of the

plate, or

$$X = \left| \int_0^L dX \right| - \left| \int_0^{-L} dX \right| , \quad (41)$$

where the indicated integration is with respect to  $t$ .

Since

$$dX < 0 \text{ for } -L < t < 0$$

and

$$dX > 0 \text{ for } 0 < t < L ,$$

equation (41) may be simplified to

$$X = \frac{3k^2 \rho}{8a^2} \int_{-L}^L t(L^2 - t^2)^{\frac{1}{2}} \frac{(t-2a)^2}{[t^2 - 2at + (4/3)a^2]^2} dt . \quad (42)$$

Now introduce the parameter  $u$  = the velocity of the vortex system and the plate and the parameter  $d$  = the length of the plate. The velocity component  $u$  is related to  $k$  by the equation

$$u = k/2b = \sqrt{3} k/2a ,$$

where  $k/2b$  is the streaming velocity necessary to bring the vortex pair to rest. The parameter  $d$  is related to  $L$  by the equation  $d=2L$ . Through elimination of  $k$ , the drag  $X$  is found from equation (42) to be given by the formula

$$X = \frac{1}{2} u^2 \rho \int_{-\frac{1}{2}d}^{\frac{1}{2}d} t \sqrt{\left(\frac{1}{2}d\right)^2 - t^2} \frac{(t-2a)^2}{[t^2 - 2at + (4/3)a^2]^2} dt. \quad (43)$$

It is customary to introduce a dimensionless drag coefficient  $C_D$  defined by the equation

$$X = C_D \cdot \frac{1}{2} \rho u^2 d.$$

Equation (43) gives the drag on half the plate; the total drag is twice this. The drag coefficient is therefore

$$C_D = (2/d) \int_{-\frac{1}{2}d}^{\frac{1}{2}d} t \sqrt{\left(\frac{1}{2}d\right)^2 - t^2} \frac{(t-2a)^2}{[t^2 - 2at + (4/3)a^2]^2} dt. \quad (44)$$

The quantity  $a$  is determined whenever the position of the vortex behind the plate is known. Photographs [18,19] indicate that the vortices assume a definite position behind the moving plate at low Reynolds numbers. The theory developed in the present section prescribes only that they lie on a curve whose equation is obtained by mapping the line

$$y = (1/\sqrt{3})x$$

onto the  $z$ -plane by

$$z = (s^2 - L^2)^{\frac{1}{2}}.$$

Another condition is required to fix their exact position on this curve. This position might be found by minimizing the drag when viscous terms are included, or it might



result from the influence of higher-order stability terms, which were neglected in the stability investigation for this flow.

Measurements taken from the photographs referred to above show that

$$z_0 = 0.70d + i(0.43d) .$$

From the equation

$$a + ib = (z_0^2 + \frac{1}{4}d^2)^{\frac{1}{2}} ,$$

$a$  is found to be equal to  $0.826d$ . For this value of  $a$  and with  $v=t/d$ , equation (44) becomes

$$C_D = 2 \int_{-\frac{1}{2}}^{\frac{1}{2}} v(\frac{1}{4}-v^2)^{\frac{1}{2}} \frac{(v - 1.652)^2}{(v^2 - 1.652v + 0.910)^2} dv ,$$

which is independent of  $d$ . This integral was evaluated numerically by electronic computer using Simpson's rule with  $n=50$ , and

$$C_D = 0.450$$

was obtained.

Experimental values of  $C_D$  have been found by Föppel [20] for values of  $d$  ranging from 10 cm to 100 cm. He obtained values of  $C_D$  from  $C_D=0.50$  for  $d=10.00$  cm to  $C_D=0.63$  for  $d=100.00$  cm, so that theoretical and experimental results agree satisfactorily for small values

of  $d$ . It is to be expected that Föppl's measurements at large values of  $d$  will be more in error than those at small  $d$  because of the necessarily finite width of his apparatus.

Karman momentum method for high speeds.--The case of a symmetrical vortex pair at rest relative to a moving cylinder apparently exists in practice [18,21] for low Reynolds numbers between 10 and 35. At Reynolds numbers greater than 50, the vortices begin to be shed and carried downstream. In the case of a flat plate situated in an infinite fluid, the vortices are shed from alternate sides and form the asymmetric wake investigated by Karman. The loss of linear momentum in the formation of a vortex wake causes the drag to increase.

After the vortex wake has formed, it is no longer possible to calculate the drag simply by integrating the pressure. By an application of Euler's momentum theorem, Karman [22] derived an approximate formula for the average drag of the vortex wake (assumed to be of semi-infinite extent in the horizontal direction) shown in Fig. 6. He first showed that the vortex street is stable when

$$b/a = (1/\pi) \arccos \sqrt{2} = 0.281 .$$

For the drag calculation Karman made the following assumptions: (i) the fully developed vortex street exists at a sufficiently great distance behind the cylinder (Fig. 6); (ii) the fluid far removed from the cylinder is at rest;

and (iii) the formation of the vortices is periodic.

Draw the rectangle ABCD (see Fig. 6) of dimensions large compared with those of the cylinder. Let  $-X-iY$  be the action of the liquid on the cylinder. Then the liquid within ABCD is acted upon by the thrust  $X+iY$  on the boundary of the cylinder and by the pressure  $p$  over the external boundary of the fluid outside. Let  $H_x+iH_y$  denote the momentum of the liquid within ABCD, and let  $F_x+iF_y$  denote the flux of momentum outwards across the boundary ABCD. Euler's momentum theorem states that the resultant force equals the time-rate of change of the total momentum. Therefore,

$$(X+iY) + i \int_C p dz = \frac{\partial}{\partial t} (H_x+iH_y) + (F_x+iF_y) ,$$

where  $C$  denotes the boundary of ABCD. Milne-Thompson [23] has carried out the evaluation of the quantities in this equation in detail, obtaining an average drag  $D$  given by

$$D = \frac{2\pi k \rho b}{a} (U-2V) + \frac{2\pi k^2 \rho}{a} ,$$

where  $U$  is the velocity of the cylinder,  $k$  is the vortex strength,  $V$  is the velocity of advance of the vortex street,  $a$  is the spacing of vortices in a single row,  $b$  is the distance between rows, and  $\rho$  is the fluid density. The vortex strength  $k$  can be eliminated by means of the equation

$$V = (k\pi/a) \tanh(b/a)\pi \quad .$$

The parameter  $b$  can be expressed in terms of  $a$  by using the stability condition  $b=0.281a$ . Introduction of a drag coefficient, defined by

$$D = C_D \cdot \frac{1}{2} \rho U^2 d \quad ,$$

where  $d$  is the diameter of the cylinder, leads to Karman's formula

$$C_D = \left[ 0.799(V/U) - 0.323(V/U)^2 \right] (a/d) \quad .$$

All parameters in this formula can be readily determined experimentally.

Karman and Rubach [24] obtained the following theoretical results based on the above formula:  $C_D=0.80$  for a flat plate and  $C_D=0.46$  for a circular cylinder. Experimental values [24] for the drag coefficients are  $C_D=0.78$  for the plate and  $C_D=0.45$  for a circular cylinder. The agreement is therefore quite good in both cases.

For a flat plate projecting from an infinite wall, the Karman asymmetric wake cannot exist, and a stable symmetric arrangement (symmetric with respect to the infinite wall) must be sought. This problem is not investigated here, although it is clear that the Karman momentum theorem will be applicable, assuming that such a vortex wake can be found.

## CHAPTER IV

## CONCLUSIONS

The example of flow past a flat plate treated in the preceding chapter indicates how the methods of conformal mapping developed in this thesis can be used to construct perfect fluid flows containing vortices. To construct a potential function for flow over the row of projections in Fig. 2, for instance, the potential function for a vortex configuration in the absence of the row of projections is stated. Then the variable is subjected to a conformal mapping of the type derived for the row of obstacles. This gives the desired potential, from which the drag may be calculated.

The usefulness of the stability theorem proved in Chapter II is that it reduces the labor involved in stability calculations. For example, a single infinite row of vortices is known to be unstable, as is a symmetrical double row [25]. Any vortex configuration, therefore, which is obtained by a conformal mapping of these arrangements must be unstable. On the other hand, the Karman asymmetrical street of vortices is stable, and it may be conformally mapped to get a stable system. Steady streaming over the infinite row of projections in Fig. 2 or Fig. 3 might cause the formation of a Karman street at low speeds

or of a staggered street of vortices, the vortices being at rest relative to the projections. At high speeds one expects each projection to shed a trail of vortices, thus increasing the total drag coefficient. The flow far enough downstream would likely be fully turbulent.

The most important practical result of Karman's investigation was his formula for the drag. It should be possible to modify this formula for the more general flows past irregular surfaces, so that the drag due to the loss of momentum in forming vortex wakes can be calculated.

The vortex problem needs to be generalized in several directions. An example of the recent trend in this field is furnished by the work of Domm [26], who investigated the spread of vorticity in a Karman street under the influence of viscosity. He found that for the case of stability the ratio of centerline width and pitch of the street is a function of the nondimensional time  $\tau = (4\nu/L^2)t$ , where  $\nu$  = kinematic viscosity,  $L$  = pitch of the vortex street, and  $t$  = time. For vanishing viscosity and also for vanishing time, the value of the spacing-ratio calculated by Karman,  $b/a = 0.28$ , was obtained. On the whole, forms of a wake more general than a Karman street have received little attention.

The methods derived and discussed in this thesis present a number of possibilities for extending the vortex-wake problem. The major drawback to using conformal

mappings is the often cumbersome form of the mapping function, for the algebraic difficulties in stability and drag calculations are more complex for complicated mapping functions. On the other hand, these mapping functions make possible the construction of perfect fluid flows which closely approximate real flows in nature. The stability theorem proved in Chapter II will simplify the stability investigation for such functions. The complexity of drag calculations remains, as does the difficulty of devising suitable vortex configurations at high Reynolds numbers. These difficulties appear to be inevitable, though not insuperable.

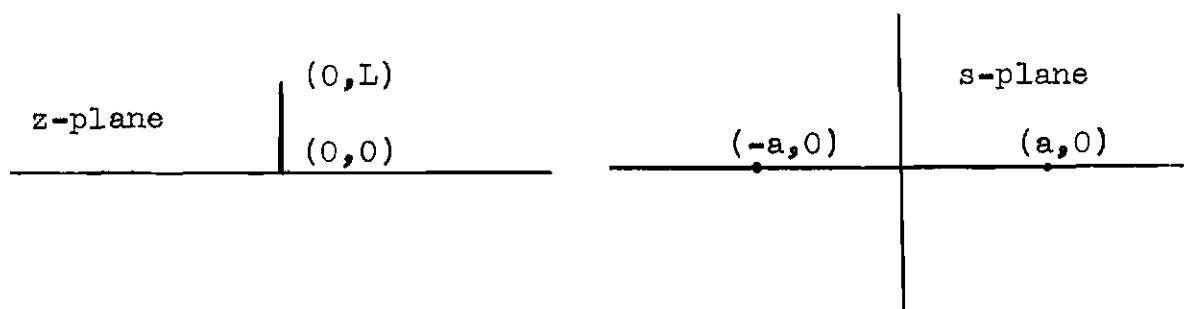


Figure 1. Single Thin Obstacle Projecting from an Infinite Wall.

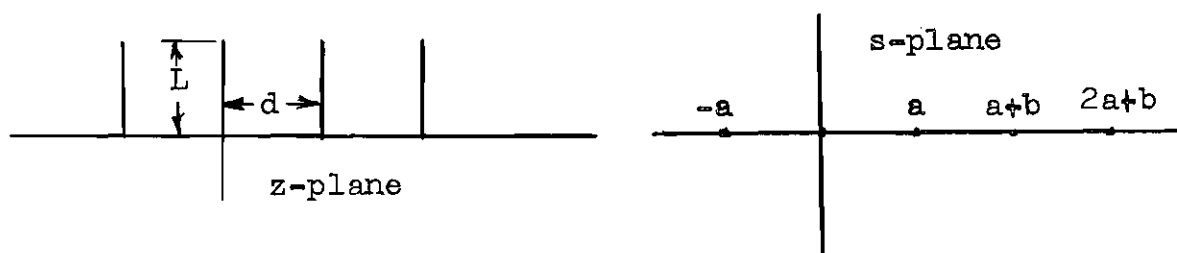


Figure 2. Infinite Row of Thin Obstacles Projecting from a Wall.



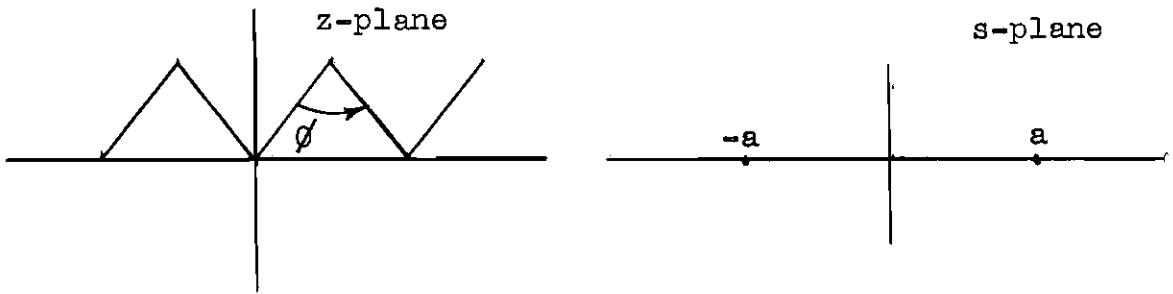


Figure 3. Infinite Saw-toothed Contour.

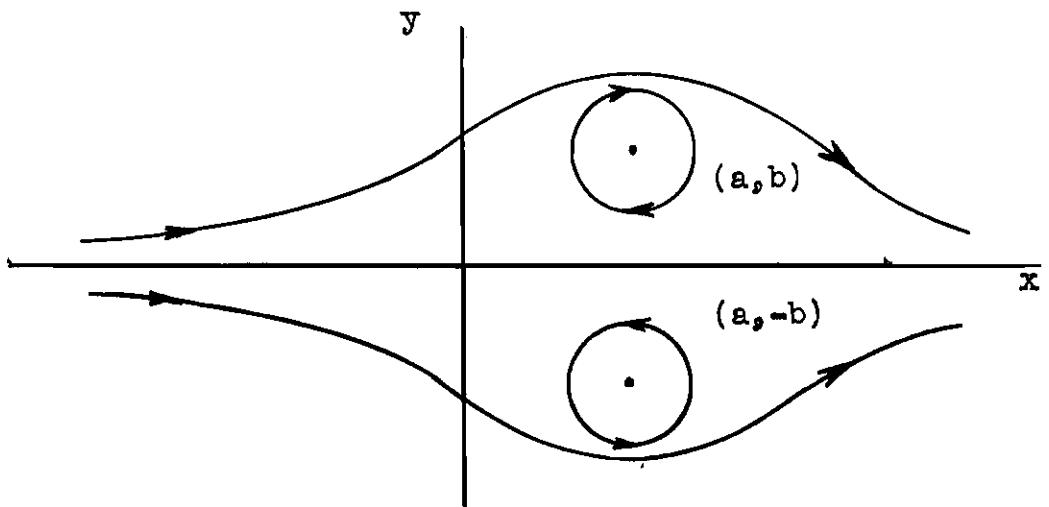


Figure 4. Vortex Pair in Steady Streaming.

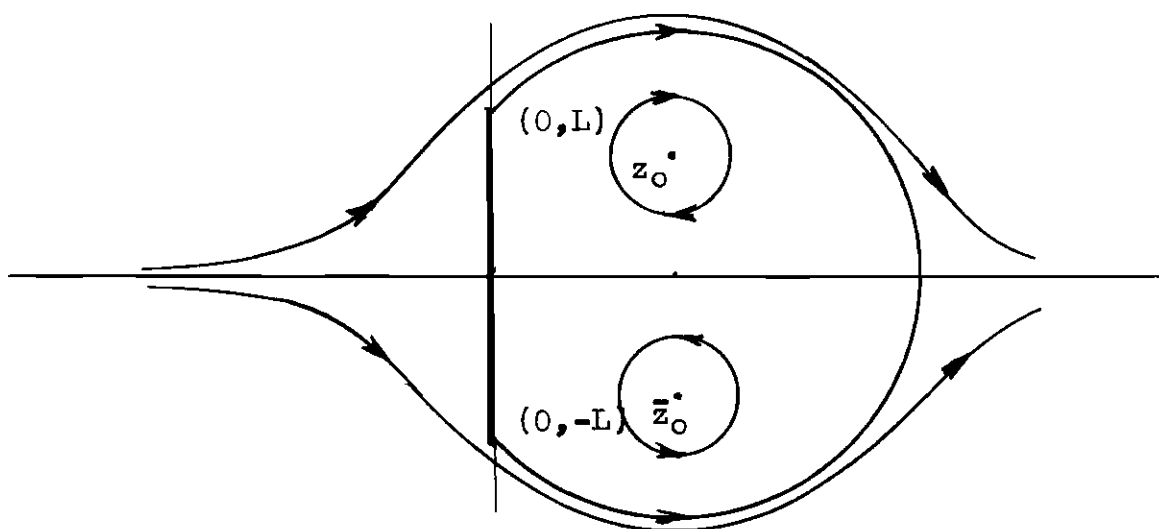


Figure 5. Vortex Pair in the Presence of a Flat Plate.

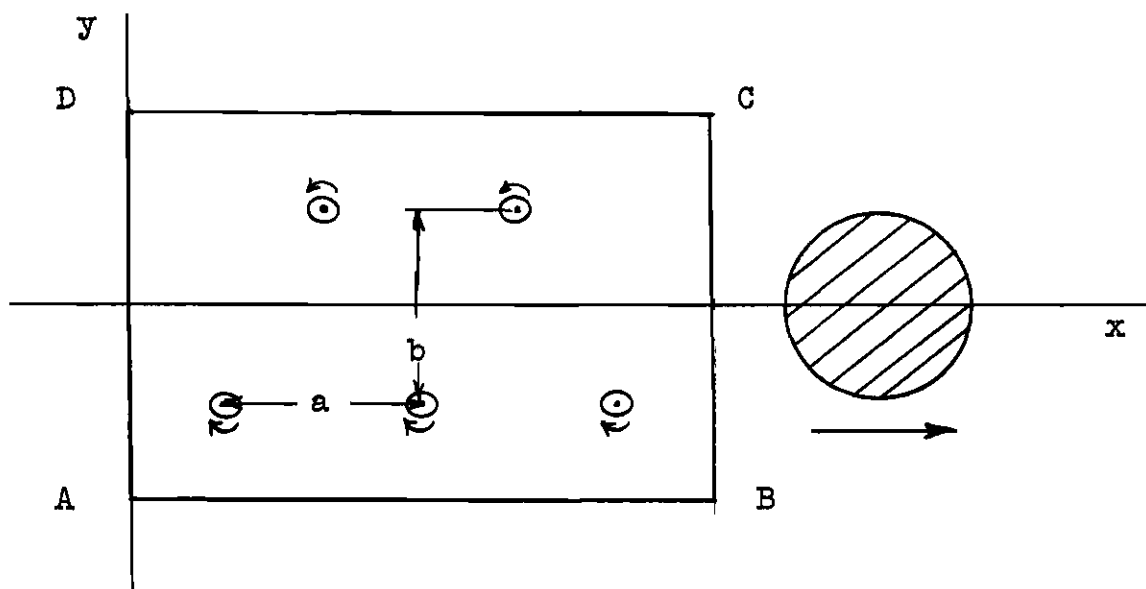


Figure 6. Karman Vortex Street

## BIBLIOGRAPHY

## LITERATURE CITED

1. Ahlfors, L. V., Complex Analysis. New York, Toronto, and London: McGraw-Hill Book Company, Inc., 1953, p. 175.
2. Nehari, Zeev, Conformal Mapping. 1st ed. New York, Toronto, and London: McGraw-Hill Book Company, Inc., 1952, p. 175.
3. Ibid., pp. 189-192.
4. Mangler, W., "Zwei Bemerkungen zum Abbildungssatz von Schwarz-Christoffel," Zeitschrift für Angewandte Mathematik und Mechanik. Vol. 18, No. 4, 1938, pp. 251-252.
5. Hobson, E. W., A Treatise on Plane Trigonometry. 5th ed. Cambridge: Cambridge University Press, 1921, p. 348.
6. Milne-Thompson, L. M., Theoretical Hydrodynamics. 3rd ed. New York: The Macmillan Company, 1955, p. 338.
7. Ibid., p. 342.
8. Birkhoff, Garrett and Zarantonello, E. H., Jets, Wakes, and Cavities. New York: Academic Press, Inc., 1957, p. 289.
9. Rosenhead, L., "The Karman Street of Vortices in a Channel of Finite Breadth," Philosophical Transactions of the Royal Society of London. Vol. 228A, 1929, pp. 275-329.
10. Milne-Thompson, L. M., op. cit., pp. 356-358.
11. Föppl, L., "Wirbelbewegung hinter einem Kreiszylinder," Sitzungsberichte der mathematisch-physikalischen Klasse der Königlich Bayerischen Akademie der Wissenschaften. 1913, pp. 1-17.
12. Goldstein, S., Modern Developments in Fluid Dynamics. Vol. II, Oxford: Clarendon Press, 1938, p. 553.

13. Karman, Theodore von, Collected Works. Vol. I, London: Butterworths Scientific Publications, 1956, pp. 324-358.
14. Ibid., p. 355.
15. Schmieden, C., "Zur Theorie der Karmanschen Wirbelstrasse," Ingenieur-Archiv. Vol. 7, 1936, pp. 337-341.
16. Rosenhead, L., op. cit., pp. 275-329.
17. Prandtl, L. and Tietgens, O., Applied Hydro- and Aerodynamics. 1st ed. New York and London: McGraw-Hill Book Company, Inc., 1934, pp. 304-305.
18. Ibid., p. 304.
19. Eck, Bruno, Technische Strömungslehre. 5th ed. Berlin-Göttingen-Heidelberg: Springer-Verlag, 1958, p. 45.
20. Föppl, L., "Ergebnisse der aerodynamischen Versuchsanstalt von Eiffel, verglichen mit den Göttinger Resultaten," Zeitschrift für Flugtechnik und Motorluftschiffahrt. Vol. 3, 1912, p. 119.
21. Goldstein, S., op. cit., p. 552.
22. Karman, Theodore von, op. cit., pp. 335-338.
23. Milne-Thompson, L. M., op. cit., pp. 364-368.
24. Karman, Theodore von and Rubach, H., "Der Mechanismus des Flüssigkeits- und Luftwiderstandes," Physikalische Zeitschrift. Vol. 13, 1912, pp. 49-59.
25. Lamb, Horace, Hydrodynamics. 5th ed. Cambridge: Cambridge University Press, 1924, pp. 208-211.
26. Domm, U., "The Stability of Vortex Streets with Consideration of the Spread of Viscosity of the Individual Vortices," Journal of the Aeronautical Sciences. Vol. 22, 1955, pp. 750-754.